

***Ab initio* study of the unusual thermal transport properties of boron arsenide and related materials**

D. A. Broido,¹ L. Lindsay,² and T. L. Reinecke³¹*Department of Physics, Boston College, Chestnut Hill, Massachusetts 02467, USA*²*NRC Research Associate at Naval Research Laboratory, Washington, D.C. 20375, USA*³*Naval Research Laboratory, Washington, D.C. 20375, USA*

(Received 21 October 2013; revised manuscript received 18 November 2013; published 11 December 2013)

Recently, using a first principles approach, we predicted that zinc blende boron arsenide (BAs) will have an ultrahigh lattice thermal conductivity, κ , of over $2000 \text{ Wm}^{-1}\text{K}^{-1}$ at room temperature (RT), comparable to that of diamond. Here, we provide a detailed *ab initio* examination of phonon thermal transport in boron arsenide, contrasting its unconventional behavior with that of other related materials, including the zinc blende crystals boron nitride (BN), boron phosphide, boron antimonide, and gallium nitride (GaN). The unusual vibrational properties of BAs contribute to its weak phonon-phonon scattering and phonon-isotope scattering, which are responsible for its exceptionally high κ . The thermal conductivity of BAs has contributions from phonons with anomalously large mean free paths ($\sim 2 \mu\text{m}$), two to three times those of diamond and BN. This makes κ in BAs sensitive to phonon scattering from crystal boundaries. An order of magnitude smaller RT thermal conductivity in a similar material, zinc blende GaN, is connected to more separated acoustic phonon branches, larger anharmonic force constants, and a large isotope mixture on the heavy rather than the light constituent atom. The striking difference in κ for BAs and GaN demonstrates the importance of using a microscopic first principles thermal transport approach for calculating κ . BAs also has an advantageous RT coefficient of thermal expansion, which, combined with the high κ value, suggests that it is a promising material for use in thermal management applications.

DOI: [10.1103/PhysRevB.88.214303](https://doi.org/10.1103/PhysRevB.88.214303)

PACS number(s): 66.70.-f, 63.20.kg, 71.15.-m

I. INTRODUCTION

We have recently examined phonon thermal transport in boron arsenide (BAs) using a first principles approach¹ and found that BAs has an exceptionally high lattice thermal conductivity, κ , over $2000 \text{ Wm}^{-1}\text{K}^{-1}$ at room temperature (RT), comparable to the highest known bulk values of the carbon crystals, diamond and graphite. For isotopically pure BAs, a κ of over $3000 \text{ Wm}^{-1}\text{K}^{-1}$ was found, again comparable to that of isotopically pure diamond. These findings were surprising, since for decades, the carbon-based crystals have been known to have κ values much higher than any other bulk material. Also, conventional guides used to estimate κ predict that the RT κ of BAs should be around $200 \text{ Wm}^{-1}\text{K}^{-1}$,^{2,3} much smaller than that of diamond. We have identified a combination of vibrational properties that contribute to the unusually high κ calculated for BAs, properties that are not present in any other material that we have examined. These are: (1) a large mass ratio of constituent atoms, which provides a large frequency gap between acoustic and optic phonons, thereby removing much of the intrinsic anharmonic scattering between acoustic and optic phonons; (2) an unusual atomic bonding, which causes a bunching together of the acoustic phonon branches and decreases intrinsic anharmonic scattering between acoustic phonons; and (3) a heavy atom (As) having only a single isotope. For large atomic mass ratio compounds, the motion of the heavy atoms dominates the heat-carrying acoustic phonon modes. Thus, compounds with both large mass ratio and isotopically pure heavy atoms show significantly weaker phonon-isotope scattering than those with heavy atoms having large isotope mixtures, regardless of the isotopic mixture of the light atoms.

Given the strikingly high κ found for BAs, the unusual underlying physical behavior, and the potential technological importance of the finding, the purpose of this paper is to provide a detailed description of the thermal transport behavior of BAs. We compare this behavior to the other boron-based III-V materials and to other relevant cubic compounds to elucidate the effect of the unique vibrational properties of BAs on thermal transport. We employ a phonon Boltzmann transport equation approach with interatomic forces determined from density functional theory to calculate κ . Calculated κ values for a large number of other materials using *ab initio* approaches have demonstrated consistently good agreement with measured values,^{1,4-14} with no adjustable parameters. This provides strong validation for the predictive capability of this first principles approach and for the surprising finding for BAs.

Cubic BAs has been fabricated, and some of its properties have been characterized previously.¹⁵⁻¹⁹ It is a semiconductor with an indirect electronic band gap measured to be about 1.5 eV and optical properties suggesting it may be a good candidate for photovoltaic applications.¹⁹ It has almost purely covalent bonding with the smallest ionicity of all III-V zinc blende compounds.²⁰ Although its thermal conductivity has not been measured, we will show that it possesses a unique combination of vibrational properties that should yield extremely high κ for high-quality crystals.

In Sec. II, we present the conceptual ingredients required to achieve high κ in nonmetallic crystals, and we highlight unusual features possessed by BAs that contribute to its high κ . Section III reviews the *ab initio* approach used to calculate κ . In Sec. IV, a broad range of calculated results for BAs is given and compared to those of other materials to illustrate the

unique combination of transport properties in BAs. A summary and conclusions are provided in Sec. V.

II. UNUSUAL PROPERTIES GIVING HIGH THERMAL CONDUCTIVITY

We note first that in semiconductors and electrical insulators, heat is carried primarily by phonons. The intrinsic lattice thermal conductivity of an infinite perfect crystal is limited by phonon-phonon scattering resulting from the anharmonicity of the interatomic potential.²¹ To lowest order, this intrinsic scattering involves three phonons.

The conventional conditions used to predict high κ for nonmetallic crystals were given by Slack.^{2,22} These are: (1) low average atomic mass, M_{avg} , (2) strong interatomic bonding, (3) simple crystal structure, and (4) low anharmonicity. Conditions (1) and (2) imply a large Debye temperature, θ_D , while condition (3) dictates a small number of atoms per unit cell. Assuming constant anharmonicity, conditions (1) and (2) suggest that κ should decrease with increasing M_{avg} and with decreasing θ_D .

These criteria are based on the theory of Liebfried and Schlömann (LS),²³ later extended by Slack^{2,22} and others.²⁴ While the LS theory has been found to give reasonable estimates of κ for a number of materials,^{2,3,22} it does not include all the properties determining the intrinsic lattice thermal conductivity. We illustrate this with the following considerations for compounds having two atoms per unit cell. Such materials have three acoustic (*a*) phonon branches and three optic (*o*) branches. Participating phonons in a three-phonon scattering process must satisfy energy and momentum conservation:

$$\omega_\lambda \pm \omega_{\lambda'} = \omega_{\lambda''} \quad \mathbf{q} \pm \mathbf{q}' = \mathbf{q}'' + \mathbf{K}, \quad (1)$$

Here, each phonon mode is labeled by the index $\lambda = (\mathbf{q}, j)$, where \mathbf{q} is the phonon wave vector and j is the phonon polarization, and ω_λ is the phonon frequency. Also, $\mathbf{K} = 0$ for normal (N) processes, and $\mathbf{K} \neq 0$ for resistive Umklapp (U) scattering. These conditions admit primarily two types of processes: (1) scattering between three acoustic phonons: $a + a \leftrightarrow a$, and (2) decay of two acoustic phonons into one optic phonon or vice versa: $a + a \leftrightarrow o$.^{25,26} We label these *aaa* and *aoa*, respectively.

One can then ask: What is required to restrict these two processes in order to increase κ ? The answer is immediately evident for *aoa* processes: If there is a large enough frequency gap between acoustic and optic phonons (*a-o* gap), then energy cannot be conserved in any *aoa* process.²⁷ This can be achieved by choosing a material with a sufficiently large mass ratio of its constituent atoms, as is well known from the diatomic linear chain model.^{28,29}

Restricting *aaa* processes is not as simple. In principle, one way to achieve this would be to make the three acoustic branches coincident throughout the Brillouin zone. This follows from a selection rule that prohibits anharmonic decay to any order of a phonon into a set of phonons of higher phase velocity, and it applies to both N and U processes.^{30,31} Thus, a hypothetical diatomic crystal with the combination of sufficiently large mass ratio and coincident acoustic branches could have extremely high thermal conductivity, limited only

by extrinsic defects such as isotopes, or crystal boundaries.^{32,33} The microscopic details of the *aaa* and *aoa* scatterings are not incorporated in the conventional conditions stated above.

However, nature does not provide crystals with coincident acoustic branches. Instead, crystals have two distinct transverse acoustic (TA) branches, TA_1 and TA_2 , and a higher-frequency longitudinal acoustic (LA) branch. It then becomes of interest to search for high- κ materials that combine the conventional criteria with the vibrational properties that tend to reduce both *aaa* and *aoa* processes. From our first principles investigations of phonon thermal transport in over two dozen materials^{1,4,5,11,12,14} and insights gained therein, we have identified BAs as having the best combination of these properties. The large As to B mass ratio of nearly 7 gives an *a-o* gap nearly equal to the highest acoustic branch phonon frequency, thus allowing no *aoa* scattering. In addition, the acoustic branches are bunched together more than in most other materials. Finally, the light boron mass, stiff covalent bonding, and small number of atoms per unit cell (two), along with relatively weak anharmonicity,³⁴ satisfy the conventional criteria for high intrinsic κ , and the isotopically pure heavy (As) atom ensures weak scattering of phonons by isotopes, as discussed below.

Before presenting supporting results, we briefly review the *ab initio* theoretical approach used to calculate κ .

III. THEORY

A. First-principles approach

The first-principles approach used here to calculate phonon thermal conductivity has been described before.^{4,5,12,14} Here, we provide a brief summary and refer readers to the referenced work for further details. We consider a cubic crystal in which a small steady-state temperature gradient, ∇T , exists. The resulting thermal current can be expressed as $\mathbf{J}_Q = (1/V) \sum_\lambda \hbar \omega_\lambda \mathbf{v}_\lambda n_\lambda$, where the sum is over all phonon modes, \mathbf{v}_λ is the phonon velocity in mode λ , and V is the crystal volume. For small ∇T , the nonequilibrium distribution function is $n_\lambda = n_\lambda^0 + n_\lambda^1$, where, $n_\lambda^0 = 1/[\exp(\hbar \omega_\lambda / k_B T) - 1]$ is the Bose factor at temperature T , and n_λ^1 is a small deviation, which is linear in the temperature gradient. A phonon lifetime can be defined through $n_\lambda^1 = -(dn_\lambda^0/dT) \sum_\alpha v_{\lambda\alpha} \tau_{\lambda\alpha} dT/dx_\alpha$, where $\tau_{\lambda\alpha}$ is the phonon lifetime in mode λ for a temperature gradient along direction α ,^{5,21} and the sum is over the Cartesian components, x , y , and z , taken to be along the cubic axes. The phonon lifetime can be determined by solving the phonon Boltzmann transport equation (BTE) using an iterative approach.^{5,35,36} We note that this transport lifetime is different from the more commonly used lifetime defined from the inverse of the total scattering rates. In the latter, momentum-conserving normal (N) processes are incorrectly treated as independent resistive processes, on the same footing as Umklapp (U) and extrinsic scattering processes. The full BTE solution corrects for this error, resulting in increased lifetimes and larger thermal conductivity. This point is discussed further in Sec. IV.

The thermal conductivity can be calculated as:

$$\kappa = \sum_\lambda C_\lambda v_{\lambda\alpha}^2 \tau_{\lambda\alpha} \quad (2)$$

where $C_\lambda = \hbar\omega_\lambda(\partial n_\lambda^0/\partial T)/V$ is the specific heat capacity per phonon mode. We note that the thermal conductivity of cubic crystals is a scalar, and we define $\kappa = \kappa_{\alpha\alpha}$.

The only inputs to the phonon BTE and resulting thermal conductivity are the harmonic and anharmonic interatomic force constants (IFCs), which are calculated *ab initio* from density functional theory^{37,38} and density functional perturbation theory³⁹ using the QUANTUM ESPRESSO package^{40,41} with norm-conserving pseudopotentials in the local density approximation (LDA). For each material, the lattice constant, a , was determined by minimization of the total ground state energy. The electronic structure calculations were typically done with 80 Ryd plane-wave cutoffs and $6 \times 6 \times 6$ Monkhorst-Pack k-point meshes. The harmonic IFCs were calculated using standard DFPT also with $6 \times 6 \times 6$ k-point meshes for each system. They were used to determine the phonon frequencies, ω_λ , eigenvectors, and velocities, v_λ . Also calculated were the effective charges and the macroscopic dielectric constants of BN, boron phosphide (BP), BAs, and boron antimonide (BSb) (referred to collectively as the BX materials). We find a small value of -0.154 for the reduced effective charge of BAs, which demonstrates its almost purely covalent bonding and a reversal from conventional anion and cation identification.²⁰ This value is in good agreement with that obtained previously.⁴²

The anharmonic IFCs were calculated using a DFT real-space supercell approach described in detail in Refs. 11 and 14. Pairs of atoms near the center of a 216 atom supercell were perturbed from the ground state configuration, and the resulting Hellmann-Feynman forces on the atoms were determined from Γ -point structure calculations. The anharmonic IFCs were determined from the numerical derivatives of these forces. We calculated anharmonic IFCs out to third nearest neighbors of the unit cell atoms.

B. Robustness of the *ab initio* model

First principles calculations of κ have demonstrated good agreement with measured thermal conductivities for a range of systems.^{1,4-14} Because of the important and surprising ultrahigh thermal conductivity of BAs, however, we performed a range of test calculations of κ of BAs and cubic (*c*) BN to verify the results. We note that *c*-BN has a large reduced effective charge, calculated to be 0.88, so long-range polar interactions may be more important in *c*-BN than in BAs, which has almost purely covalent bonding. We have tested the following: (1) inclusion of up to third nearest neighbors for the real-space anharmonic IFCs (results for this case are presented in Sec. IV), (2) inclusion of up to fifth nearest neighbors for the real-space anharmonic IFCs, (3) a reciprocal space approach that includes anharmonic IFCs up to seventh nearest neighbors^{4,5,43} and long-range Coulomb interactions,⁴⁴ (4) an approach using harmonic and anharmonic IFCs determined in the generalized gradient approximation (GGA) with ultrasoft pseudopotentials and a nonlinear core correction, and including up to third nearest neighbors for the real-space anharmonic IFCs, and (5) two different approaches to solve the phonon BTE—a phase space search approach⁵ and an adaptive Gaussian smearing approach.^{45,46} For BAs, we find that the ultrahigh κ obtained using method (1) is robust against

calculational differences in (2), (3), (4) and (5). For example, at RT, we find that the isotopically pure thermal conductivity, κ_{pure} , of BAs from method (1) is $3170 \text{ Wm}^{-1}\text{K}^{-1}$.⁴⁷ Methods (2) and (3) give only a 1% reduction to this value. Methods (4) and (5) give a 4% and 0.5% increase to this value, respectively. For *c*-BN, we find more substantial differences. Using method (1), we calculate $\kappa_{\text{pure}} = 2145 \text{ Wm}^{-1}\text{K}^{-1}$ for *c*-BN. Method (2) gives a 4% reduction to this value. Method (3) gives a 1% increase to this value. Method (4) gives a 14% reduction, and method (5) gives a 4% increase to this value. The decrease in κ_{pure} for *c*-BN using method (4) is due to known differences between LDA and GGA calculations, which tend to overbind and underbind atoms, respectively. As a result, the GGA calculations give optic phonon branches lower than the LDA calculations, and lower than experiment. This gives enhanced *aao* scattering and reduces κ .^{1,12,14}

IV. RESULTS AND DISCUSSION

For high-quality semiconductors and insulators, the dominant phonon scattering mechanisms around RT are intrinsic three-phonon scattering and scattering of phonons by isotopes. In the following, we consider only these two scattering mechanisms. Expressions used here for the phonon-phonon and phonon-isotope scattering rates have been published previously.^{5,11,12,43,48,49} We first present results for the intrinsic κ of isotopically pure materials.

A. Intrinsic thermal conductivity

Figure 1 shows the calculated intrinsic κ (κ_{pure}) for isotopically pure *c*-BN, BP, BAs, BSb, and diamond as a function of temperature. Around and above RT, the intrinsic κ for BAs is considerably higher than those for the other BX systems, reaching a RT value of around $3200 \text{ Wm}^{-1}\text{K}^{-1}$,

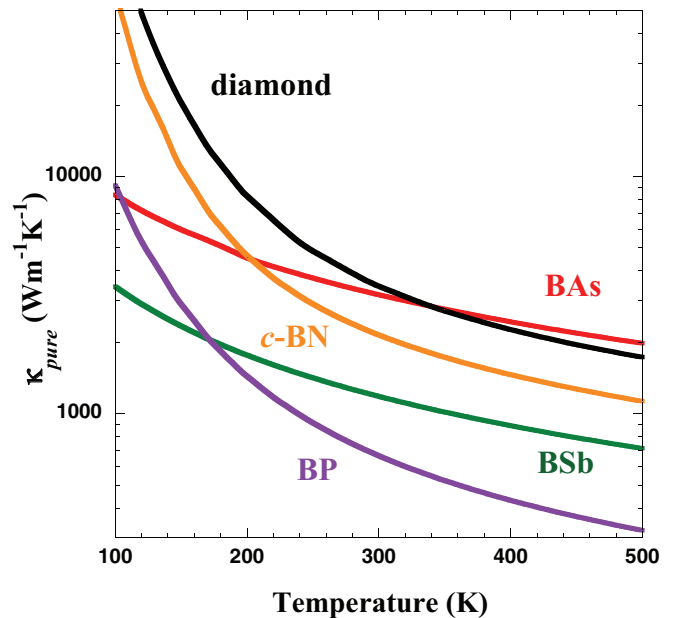


FIG. 1. (Color online) Intrinsic thermal conductivity, κ_{pure} , as a function of temperature for *c*-BN (orange), BP (purple), BAs (red), and BSb (green). Also shown is the κ_{pure} of diamond (black).

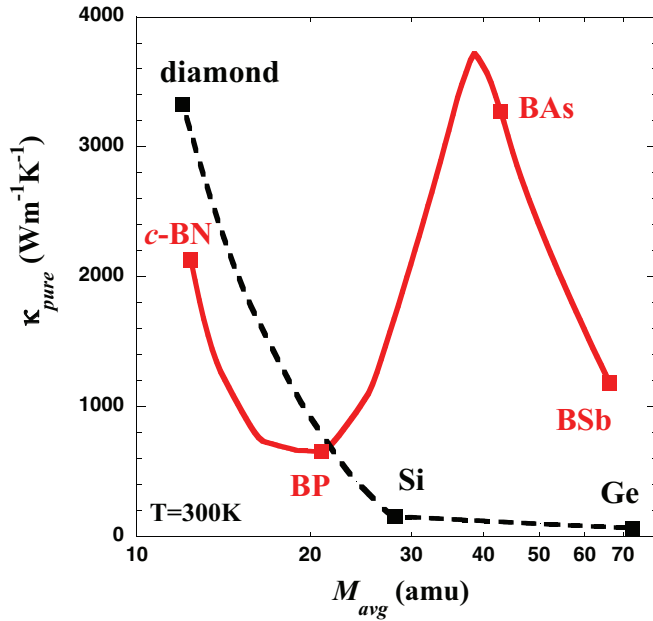


FIG. 2. (Color online) Calculated RT κ_{pure} (solid red curve) vs. M_{avg} for BX crystals where the properties (atomic masses, interatomic force constants, effective charges, dielectric constants) of pairs of group V atoms (i.e., X in BX) are averaged continuously using their relative concentrations in going from N to P to As to Sb. Also shown is the κ_{pure} calculated by averaging the properties of elemental group IV materials spanning diamond to silicon (Si) to germanium (Ge) (dashed black curve). Qualitatively similar curves can be obtained plotting κ_{pure} against the Debye temperature, θ_D . The calculated κ_{pure} values for the BX materials are shown by the solid red squares, and those for the elemental materials (diamond, Si, and Ge) are shown by the black squares.

which is comparable to that of diamond, and even larger than that of diamond above RT. This result is not predicted using the conventional guidelines that direct the search for high- κ materials. For example, in comparing with diamond, the M_{avg} of BAs is over three times larger, the calculated θ_D of BAs is about three times smaller, and the anharmonicity in the two materials is roughly the same by conventional measure.^{1,34}

The unusual behavior of κ in BAs and the other BX materials is illustrated in Fig. 2, where the RT κ_{pure} is given as a function of M_{avg} for the BX materials and for the elemental materials: diamond, Si, and Ge. The solid curve segments are obtained by averaging relevant physical properties (atomic masses, force constants, lattice constants, etc.) of each pair of materials at the segment end points. The curve for the elemental materials follows the typical behavior, with κ_{pure} decreasing monotonically with increasing M_{avg} . This is associated with the heavier mass and reduced θ_D , which result in decreased acoustic phonon velocities and frequencies and with increased phonon-phonon scattering by increasing phonon populations. The BX curve initially follows a similar trend, with κ_{pure} dropping from *c*-BN to BP. However, the curve then rises from BP to peak at around $3700 \text{ Wm}^{-1}\text{K}^{-1}$, with BAs appearing very near this peak before dropping again to BSb. We found the same unusual behavior for κ_{pure} in the beryllium-VI cubic compounds, although with lower thermal conductivities.⁴⁸

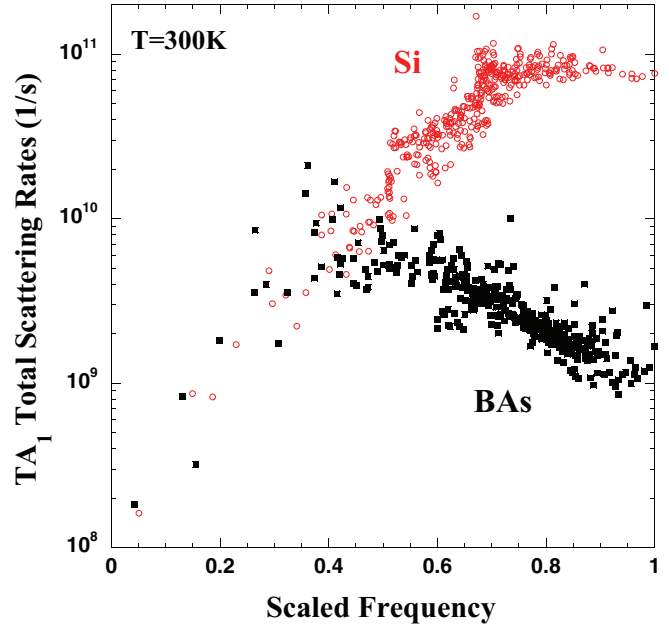


FIG. 3. (Color online) Total anharmonic three-phonon scattering rates for the TA_1 branch at $T = 300 \text{ K}$ for BAs (solid black squares) and Si (hollow red circles) as a function of frequency. The phonon frequencies are scaled by the highest TA_1 frequency for each material. The total scattering rates increase monotonically with increasing frequency in Si, while in BAs, they decrease with increasing frequency in the mid- to high-frequency range.

Underlying this surprising behavior are features of BAs in particular and the BX materials in general that conspire to cause weak intrinsic thermal resistance. First, the light boron mass keeps the average atomic mass relatively small, and this, combined with the stiff bonding, gives unusually high-frequency scales in the BX materials compared to many other materials. Second, the large mass difference between As and B ($M_{\text{As}}/M_{\text{B}} = 6.93$) produces a large gap between acoustic and optic phonon branches (the *a-o* gap) (see Fig. 11 for the phonon dispersion of BAs, and fig. 3 in Ref. 50). Finally, in the BX materials and diamond, the acoustic branches are closer together than they are in Si. This is particularly noticeable along the $\Gamma \rightarrow K$ direction, where the TA_2 and LA branches come quite close (See Fig. 2 in Ref. 1).

B. Intrinsic phonon-phonon scattering rates

The larger *a-o* gap and the bunching of the acoustic branches have a profound effect on the intrinsic anharmonic scattering rates of BAs. To illustrate this, Figs. 3 and 4 compare these scattering rates against frequency for phonons from the TA_1 branch in Si and BAs. The frequencies are obtained on a fine mesh of \mathbf{q} points in the irreducible wedge of the Brillouin zone. The spread in values at each frequency reflects the \mathbf{q} -dependent anisotropy in the scattering rates. This comparison is useful since BAs and Si have similar frequency ranges and acoustic velocities for their acoustic branches. Figure 3 shows the total scattering rates, while Fig. 4 gives the scattering rate breakdown by the different combinations of *a* or *o* phonons. For ease of comparison, frequencies are scaled by the maximum calculated acoustic

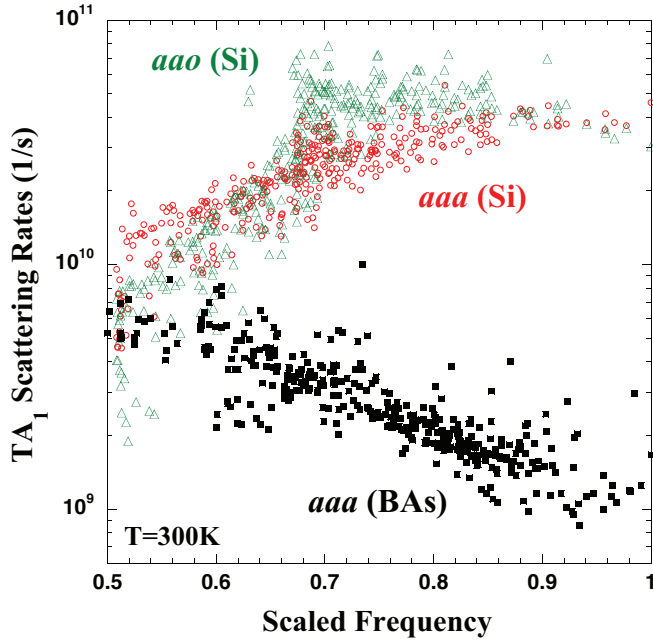


FIG. 4. (Color online) Anharmonic three-phonon scattering rate contributions for the TA₁ branch at $T = 300$ K from the *aao* and *aaa* processes as a function of frequency. Solid black squares give the *aaa* contributions for BAs. Hollow red circles (green triangles) give the *aaa* (*aao*) contributions for Si. The phonon frequencies are scaled by the highest TA₁ frequency for each material.

phonon branch frequency for each material. At low frequencies (not shown in Fig. 4), *aaa* and *aao* contributions to the intrinsic scattering rates are similar and dominant in both materials. In Si, at higher frequencies, *aaa* and *aao* processes dominate and are comparable in strength. The total scattering rates shown in Fig. 3 (i.e., *aaa* + *aao* + *aoo*) increase monotonically with increasing frequency in Si. In contrast, the scattering rate behavior in BAs is quite different. For BAs, the *aao* processes are absent due to the large *a-o* gap. Further, with increasing frequency, the *aaa* processes in BAs first increase and then *decrease* in the mid- to high-frequency range of the acoustic phonon spectrum, becoming more than an order of magnitude smaller in BAs than those for Si approaching the highest-frequency region.

Another difference is seen by examining the respective strengths of the Umklapp (U) scattering rates in Si and BAs. Acoustic phonons carry the majority of the heat due to their larger acoustic velocities and larger phonon populations compared to optic phonons. Umklapp scattering, which is directly responsible for the thermal resistance, typically occurs for higher-frequency acoustic phonons for which wave vectors are a substantial fraction of the Brillouin zone.²¹ Figure 5 gives the ratio of the anharmonic scattering rates for U processes to the total intrinsic scattering rates (U + N) as a function of frequency for phonons in the TA₂ branch. Phonon frequencies are again scaled by the largest frequency in that branch. In the region of small frequencies, N scattering is prevalent, and U scattering is weak for both materials, as expected. For higher frequencies, the resistive U scattering becomes dominant in Si. In contrast, the U scattering is relatively weak in BAs, even at higher frequencies. This is

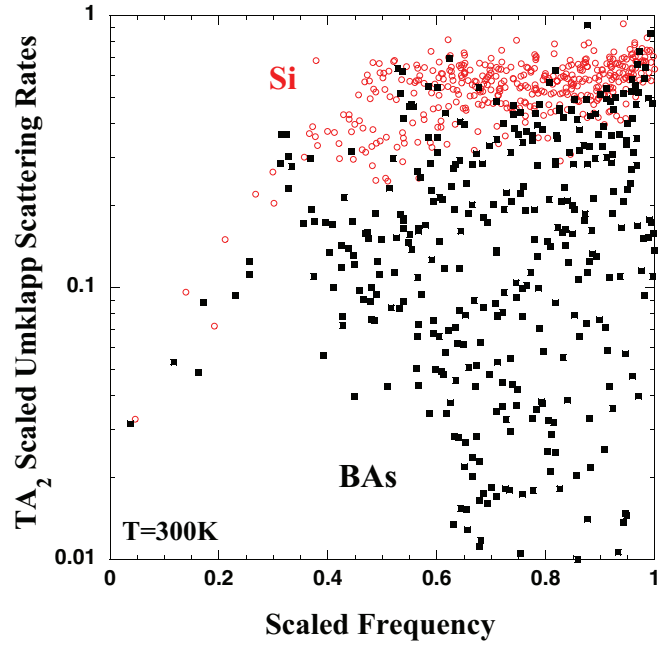


FIG. 5. (Color online) Umklapp scattering rates for the TA₂ branch at RT as a function of frequency for BAs (solid black squares) and Si (hollow red circles). The Umklapp scattering rates are scaled by the total anharmonic three-phonon scattering rates, and the phonon frequencies are scaled by the highest TA₂ frequency for each material. The weaker Umklapp scattering ratio for BAs at higher frequencies is particularly striking since the total BAs intrinsic scattering rates are already much smaller than those in Si.

particularly striking given that the total intrinsic scattering rates for BAs in this frequency range are already weak, as seen in Figs. 3 and 4.

Insight into the weak intrinsic scattering rates of the acoustic phonons in BAs is gained from examination of the two-phonon density of states:

$$D_j^\pm(\mathbf{q}) = \sum_{j'j''} \int d\mathbf{q}' \delta(\omega_j(\mathbf{q}) \pm \omega_{j'}(\mathbf{q}') - \omega_{j''}(\mathbf{q} \pm \mathbf{q}' - \mathbf{K})) \quad (3)$$

which gives a measure of the phase space available for three-phonon scattering per phonon mode, $\Delta_j(\mathbf{q}) = D_j^+(\mathbf{q}) + D_j^-(\mathbf{q})/2$.⁵¹ Figure 6 compares $\Delta_{TA_2}(\mathbf{q})$ for Si and BAs for a fine \mathbf{q} mesh in the irreducible wedge. As in Figs. 3–5, the spread in values reflects the \mathbf{q} -anisotropy of this phase space. The horizontal axis again gives phonon frequency scaled by the largest TA₂ frequency for a mesh of \mathbf{q} points taken from the irreducible wedge of the Brillouin zone. For small frequency corresponding to small \mathbf{q} near the center of the Brillouin zone, the TA₂ phase space for three-phonon scattering in BAs is comparable to or larger than that of Si. However, for higher frequencies, this phase space decreases rapidly in BAs while staying roughly constant in Si. The large *a-o* gap in BAs has removed all *aao* processes, which are prevalent in Si (see Fig. 4). Thus, the rapid phase space decrease in BAs arises from a decrease in *aaa* processes, which is a direct consequence of the bunching of acoustic branches. As noted in Sec. II, *aaa* processes become forbidden throughout most, if not all, of

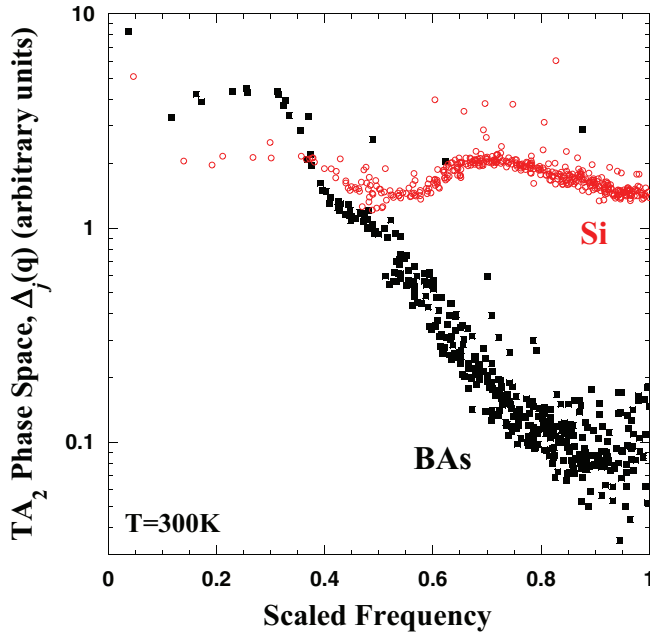


FIG. 6. (Color online) Phase space for three-phonon scattering per phonon mode for the TA_2 branch at RT as a function of scaled frequency for BAs (solid black squares) and Si (hollow red circles), as defined from the two-phonon density of states, Eq. (3). The rapid phase space decrease in BAs arises from a decrease in aaa processes resulting from the bunching together of the acoustic branches.

the Brillouin zone if the acoustic branches coincide.^{30,31} As the acoustic branches approach this limit, the phase space for three-phonon scattering decreases correspondingly. While this limit does not actually occur in any material, the bunching of the acoustic branches is quite noticeable in the mid- to high-frequency range in BAs, the other BX materials, and in diamond (see Fig. 11 herein, Fig. 3 in Ref. 50, and Fig. 1 in Ref. 5).⁵² We find that the dominant three-phonon aaa scattering processes in the elemental group IV and zinc blende III–V materials that we have studied involve two TA phonons and one LA phonon: $TA_{1,2} + TA_{1,2} \leftrightarrow LA$. The bunching together of the three acoustic branches in BAs compared to Si (see Fig. 2 in Ref. 1) throughout the Brillouin zone reduces the phase space for this scattering, as seen in Fig. 6.

An additional consequence of the acoustic branch bunching is the weakening of the three-phonon scattering matrix elements, $|\Phi_{\lambda\lambda'\lambda''}|^2$ (see Eq. 8 in Ref. 5), for the allowed aaa processes. Since the acoustic branches are similar in energy due to the bunching, a phonon with frequency ω_λ in the higher-frequency range can decay via a three-phonon process into two phonons, one with a similar high frequency, $\omega_{\lambda''}$, and one with a small frequency, $\omega_{\lambda'}$, and thus small wave-vector magnitude, q' . In this case, the scattering matrix elements scale as $|\Phi_{\lambda\lambda'\lambda''}|^2 \sim q'^2$.⁵³ As the branches bunch together, q' and the matrix elements get smaller, and the resulting aaa scattering becomes weaker. Interestingly, there is a competition between this matrix element reduction and an increase in the scattering rate prefactor terms (see Eq. 8 in Ref. 5), which contain $n_{\lambda'}^0/\omega_{\lambda'} \sim (1/q')^2$ for acoustic branches with small q' . Also, other factors such as the magnitudes of the anharmonic IFCs and the atomic masses enter into determining the scattering

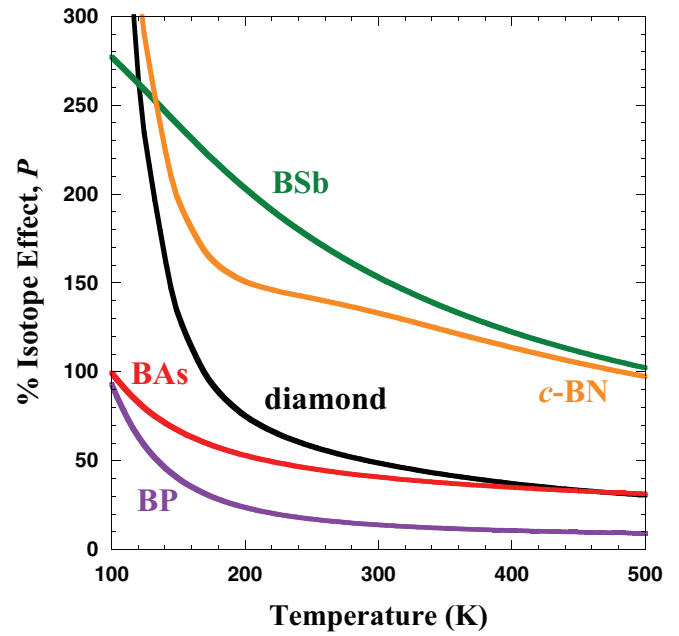


FIG. 7. (Color online) Calculated isotope effect, $P = 100(\kappa_{\text{pure}}/\kappa_{\text{nat}} - 1)$, as a function of temperature for c -BN (orange), BP (purple), BAs (red), BSb (green), and diamond (black).

rates. Careful calculations are required to determine the scattering behavior for a given material.

C. Temperature dependence

The intrinsic thermal conductivities of BAs and BSb have weaker temperature dependence than those of the other materials in Fig. 1. For low temperature, aaa scattering is weak in all materials. In this case, the intrinsic κ values follow the prediction of conventional guidelines; i.e., materials with lighter atoms and stiffer bonds have higher intrinsic κ . Thus, at $T = 100$ K, the intrinsic thermal conductivities are ordered: diamond, c -BN, BP, BAs, and BSb. With increasing temperature, the onset of $a-o$ scattering in diamond, BN, and BP causes a faster drop in κ for these materials. At $T = 400$ K, the intrinsic thermal conductivities are reordered: BAs, diamond, c -BN, BSb, and BP.

D. Thermal conductivity with natural isotope mixtures

Phonon scattering by naturally occurring isotopes reduces κ . The relative strength of the phonon-isotope scattering compared to the intrinsic phonon-phonon scattering can be characterized by the percent isotope effect: $P = 100(\kappa_{\text{pure}}/\kappa_{\text{nat}} - 1)$. Excluding materials with the highest thermal conductivities, phonon-isotope scattering is typically much weaker than intrinsic phonon-phonon scattering around RT. As a result, the corresponding P is small. For example, in Si, the RT P is about 8%, while in GaAs, it is about 4%. In contrast, for high-thermal-conductivity materials such as diamond, the intrinsic phonon-phonon scattering is unusually weak. Then, scattering of phonons by isotopes can be comparable to the intrinsic scattering and can significantly reduce κ .

Figure 7 plots the calculated P as a function of temperature for the BX materials and for diamond. Although natural carbon

has a relatively small isotope mix (98.9% ^{12}C , 1.1% ^{13}C), the P value for diamond is large (50% at RT) because the stiff covalent bonding and light atomic mass give a high phonon frequency scale. As a result, RT is an effectively low temperature compared to the Debye temperature in diamond, and the intrinsic phonon-phonon scattering is correspondingly weak. Around and above RT, P for c -BN is larger than that of diamond (130% at RT for c -BN), even though its frequency scale is lower. This difference reflects primarily the larger isotope mix in boron (19.9% ^{10}B , 80.1% ^{11}B) compared to that in carbon, which causes stronger phonon-isotope scattering in c -BN. In contrast, the P for BAs around and above RT is comparable to that of diamond and becomes considerably smaller than that of diamond well below RT. This is at first surprising since the large boron isotope mix also occurs in BAs as it does in c -BN. The weak phonon isotope scattering in BAs results from the large As to B mass ratio, which causes the motion of the heavy (and in this case, isotopically pure) As atoms to dominate for high-frequency acoustic phonons.^{1,30,48,49} For c -BN, the constituent masses are similar, and the motion of the boron atoms plays a significant role in the phonon-isotope scattering of the acoustic phonons. The much larger isotope effect for BSb compared to BAs reflects the large isotope mix on the heavy Sb atoms.

With decreasing temperature, the isotope effect in diamond increases more rapidly than in BAs. This reflects in part the weakening ao scattering in diamond, which causes the intrinsic κ to rise faster than in BAs, as seen in Fig. 1. In addition, the high-frequency scale in diamond makes N scattering more important at low temperature than in BAs.

E. Thermal conductivity accumulation

New measurement techniques are able to extract the accumulation of thermal conductivity as a function of the phonon mean free path (mfp),^{54–56} and good agreement between *ab initio* calculations⁸ and measurements have been obtained for Si.^{55,56} This accumulation provides insight into the nature of thermal transport in materials. We define the mfp of a phonon in mode λ as $|\mathbf{v}_\lambda| \tau_{\lambda z}$, with z along the direction of a cubic axis and temperature gradient. The thermal conductivity accumulation is:

$$\kappa_{\text{acc}}(l) = \sum_{\lambda} C_{\lambda} v_{\lambda z}^2 \tau_{\lambda z} \theta(l - |\mathbf{v}_\lambda| \tau_{\lambda z}) \quad (4)$$

where $\theta(x)$ is the Heaviside step function, which is zero (one) for $x < 0$ ($x > 0$). The term $\kappa_{\text{acc}}(l)$ sums the fraction of heat carried by phonons with mfps smaller than l . Figure 8 shows $\kappa_{\text{acc}}(l)$ at RT for Si and BAs with naturally occurring isotope concentrations. The values are scaled by the total κ_{nat} for each material. For Si (thick black curve), the accumulation is spread over more than three orders of magnitude of mfps, with 80% lying in the wide range $0.05 \mu\text{m} < l < 20 \mu\text{m}$, and with the 50% total accumulation point occurring near $0.6 \mu\text{m}$. These results are in good agreement with previous *ab initio* calculations^{8,46} and with measured values.⁵⁶ On the other hand, for BAs, the accumulation is over a much narrower range: 80% of the accumulation occurs for $1.2 \mu\text{m} < l < 3.3 \mu\text{m}$, and it is shifted to larger mfps, with the 50% accumulation point occurring at $2 \mu\text{m}$. These differences

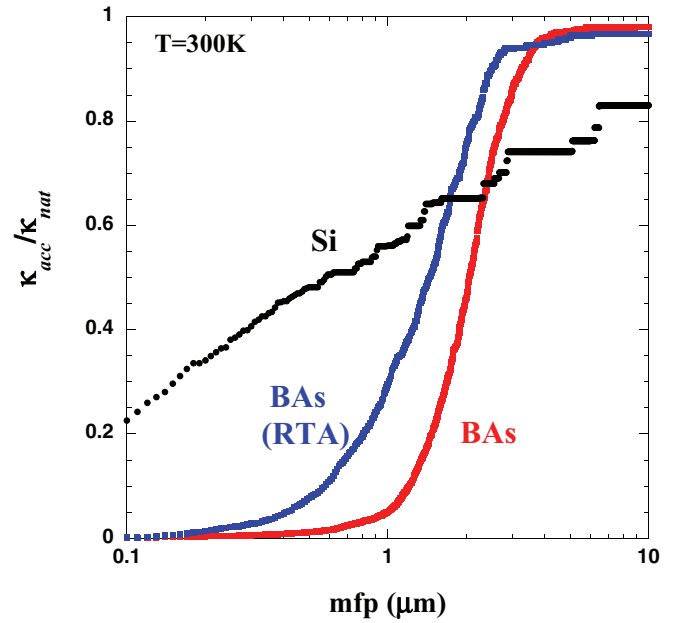


FIG. 8. (Color online) Calculated thermal conductivity accumulation, $\kappa_{\text{acc}}(l)$, at $T = 300 \text{ K}$ for naturally occurring isotope concentrations as a function of phonon mean free path for BAs (red curve) and Si (black curve). $\kappa_{\text{acc}}(l)$ is scaled by the total κ_{nat} in this case. The blue curve gives $\kappa_{\text{acc}}(l)/\kappa_{\text{nat}}$ for BAs in the RTA.

can be understood qualitatively as follows: For Si, the main contributions to κ come in the frequency range below 6 THz, where these contributions are roughly constant (see Fig. 3 in Ref. 1). The increasingly strong scattering rates (see Fig. 3 for TA_1 phonons) cause acoustic phonon scattering times $\tau_{\lambda z}$ to decrease rapidly over this frequency range, giving the observed wide range of mfps contributing to the Si thermal conductivity accumulation. In contrast, acoustic branch bunching in BAs gives decreased scattering rates in the middle to high range of acoustic phonon frequencies (see Fig. 3 for TA_1 phonons), which keep the corresponding $\tau_{\lambda z}$ larger than those in Si and within a narrower lifetime range. This focuses accumulation contributions at larger mfps and within the narrow mfp range seen in Fig. 8.

The blue curve in Fig. 8 shows the scaled $\kappa_{\text{acc}}(l)$ for BAs in the relaxation time approximation (RTA) to the phonon BTE. In the RTA, the phonon lifetimes are taken from Matheissen's rule: $1/\tau_{\lambda}^{\text{RTA}} = 1/\tau_{\lambda}^{\text{N}} + 1/\tau_{\lambda}^{\text{U}} + 1/\tau_{\lambda}^{\text{iso}}$, where $1/\tau_{\lambda}^{\text{N}}$ and $1/\tau_{\lambda}^{\text{U}}$ are the intrinsic scattering rates for Normal and Umklapp, respectively. This incorrectly treats N processes as resistive, which artificially increases the thermal resistance and shifts the accumulation to smaller mfps. Further, the calculated κ_{nat} within the RTA is about 40% smaller than the full solution to the BTE. This highlights the importance of implementing the full iterative solution to the BTE.

Figure 9 compares the $\kappa_{\text{acc}}(l)/\kappa$ values for BAs, diamond, and c -BN with naturally occurring isotope concentrations (thicker curves) with those for the isotopically pure materials (thinner curves). For the pure case, the accumulation in diamond occurs at smaller mfps than for BAs. This seems at first contradictory, since the RT κ_{pure} values for diamond and BAs are about the same. The explanation is as follows: The acoustic phonon group velocities in diamond are larger

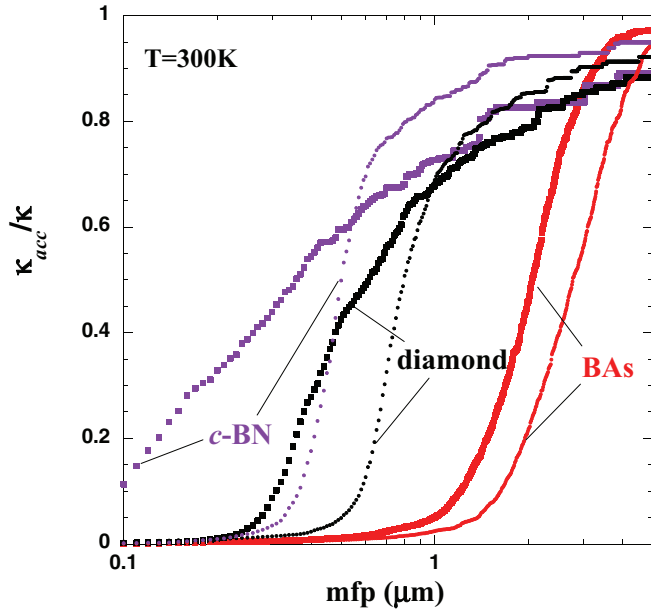


FIG. 9. (Color online) Calculated $\kappa_{acc}(l)/\kappa$ at $T = 300$ K for naturally occurring isotope concentrations (thick curves) and isotopically pure (thin curves) BAs (red), diamond (black), and *c*-BN (purple) as a function of phonon mean free path.

than those in BAs. However, the largest contributions to the diamond κ occur at high frequencies, where the acoustic phonon lifetimes are relatively small. On the other hand, the largest κ contributions in BAs come in a narrow region of lower frequencies, where the corresponding lifetimes are larger. The mfp for mode λ , $|\mathbf{v}_\lambda| \tau_{\lambda z}$, is linear in the velocity, but the thermal conductivity integrand is quadratic in the velocity (see Eq. (2)). This larger velocity weighting gives diamond similar κ to BAs, even though the contributing mfps are smaller.

The effect on $\kappa_{acc}(l)$ of phonon-isotope scattering in diamond and *c*-BN is markedly different than it is in BAs. In diamond and *c*-BN, the acoustic phonon-isotope scattering rates are weak at low frequency and increase rapidly and monotonically with increasing frequency, flattening out near the maximum acoustic phonon frequencies, where they approach (diamond) or exceed (*c*-BN) the RT phonon-phonon scattering rates. As a result, contributions from the higher-frequency (small mfp) phonons are suppressed and shifted to even smaller mfps, while the fractional contributions to $\kappa_{acc}(l)$ increase for the lower-frequency (large mfp) phonons, as seen in Fig. 9. Similar behavior has been noted in $\text{Mg}_2\text{Si}_x\text{Sn}_{1-x}$ alloys.¹¹ In BAs, the acoustic phonon-isotope scattering rates are weak, with roughly constant peak values in a narrow frequency range (see Fig. 13 for TA_1 phonons) that coincides with the peak contributions to κ_{pure} (see Fig. 3 in Ref. 1). This causes the full accumulation curve to be rigidly shifted to smaller mfp. The weakness of this isotope scattering ensures that this shift is relatively small.

The large lifetimes in the narrow region of higher acoustic phonon frequencies give an unusual distribution of per-branch contributions to the thermal conductivity in BAs. For conventional high- κ materials, the RT per-branch contribu-

tions decrease with increasing frequency, i.e., in going from TA_1 to TA_2 to LA. Thus, for diamond (*c*-BN), the fractional contributions to the RT κ_{nat} from these three branches are: 0.41 (0.45), 0.34 (0.31), and 0.25 (0.24). This trend is a consequence of the high-frequency scales in diamond and *c*-BN (maximum acoustic phonon frequencies for diamond and *c*-BN are 5.8 and 4.9 times larger than the RT thermal energy, respectively), which give a reduction in RT acoustic phonon population with increasing frequency. In contrast, the acoustic phonon frequency range in BAs extends to only 50% higher phonon energy than the RT thermal energy, and roughly the same per-branch contributions might be expected. However, for BAs, the fractional contributions to the RT κ_{nat} for TA_1 to TA_2 to LA are: 0.25, 0.49, and 0.26, which show that the TA_2 contribution is twice as large as those from TA_1 and LA. This anomalously large TA_2 contribution occurs because of a coincidence of large TA_2 group velocities with large TA_2 phonon lifetimes.

To summarize this section, the majority of heat transported in BAs comes from large mfp phonons within a narrow range of mfps. The accumulation of thermal conductivity as a function of phonon mfp in BAs is not much affected by phonon-isotope scattering.

F. Sensitivity to boundary scattering

The large mfps of phonons carrying heat in BAs and the narrow range over which they are distributed make the acoustic phonons sensitive to scattering from crystal boundaries. An estimate of this effect can be obtained by including a boundary scattering rate:²¹ $1/\tau_\lambda^b = |\mathbf{v}_\lambda|/L$, where L gives a qualitative measure of the crystal size. Figure 10 compares the RT κ_{nat} values for BAs with those of diamond as a function of L . Below about 10 μm , the κ_{nat} for BAs drops more rapidly than that for diamond. Diamond also has κ accumulation over a narrow

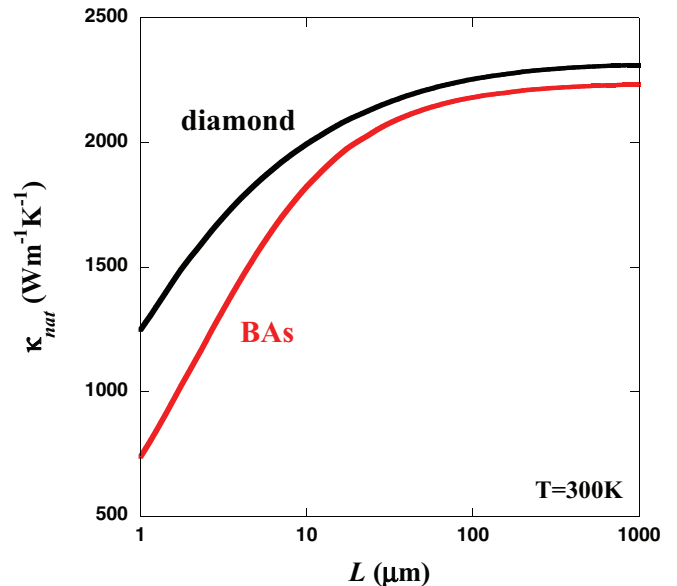


FIG. 10. (Color online) Calculated κ_{nat} at $T = 300$ K for diamond (black curve) and BAs (red curve) as a function of boundary scattering length, L , which gives a qualitative measure of the crystal size. The κ of BAs is more sensitive to scattering from crystallite boundaries.

range of mfps,^{46,57} but it is concentrated at mfps less than half those for BAs (50% accumulation occurs at around 0.8 μm for diamond). As a result, the diamond thermal conductivity drops less rapidly with the boundary scattering length than does that of BAs.

G. Coefficient of thermal expansion

Materials used for passive cooling applications must have coefficients of thermal expansion (CTEs) that closely match those of the sensitive electronics they are designed to cool in order to prevent thermal stresses. Therefore, it is important to examine the CTE of BAs compared to commonly used materials in microelectronic devices, in particular silicon. Within the quasiharmonic approximation, the CTE is given by:

$$\text{CTE} = \frac{1}{3B_0} \sum_{\lambda} C_{\lambda} \gamma_{\lambda} \quad (5)$$

where B_0 is the bulk modulus determined from the harmonic IFCs, and γ_{λ} is the mode Grüneisen parameter, which can be expressed as:⁵⁸

$$\begin{aligned} \gamma_{\lambda} &= -\frac{V}{\omega_{\lambda}} \frac{d\omega_{\lambda}}{dV} \\ &= -\frac{1}{6\omega_{\lambda}^2} \sum_k \sum_{l'k'} \sum_{l''k''} \sum_{\alpha\beta\gamma} \Phi_{\alpha\beta\gamma}(0k, l'k', l''k'') \\ &\quad \times \frac{e_{\alpha k}^{\lambda*} e_{\beta k'}^{\lambda} e_{\gamma k''}^{\lambda}}{\bar{m}_k \bar{m}_{k'}} e^{i\mathbf{q}\cdot\mathbf{R}_l} r_{l''k''\gamma} \end{aligned} \quad (6)$$

where lk designates the k th atom in the l th unit cell, $e_{\alpha k}^{\lambda}$ and \bar{m}_k are the α th component of the phonon eigenvector and isotope-averaged atomic mass of that atom, respectively, and the terms $\Phi_{\alpha\beta\gamma}(lk, l'k', l''k'')$ are the third-order anharmonic IFCs. \mathbf{R}_l and $r_{lk\alpha}$ are the lattice vector and the α th component of the vector locating the k th atom in the l th unit cell. The calculated values obtained for B_0 are 1.57 Mbar (BAs) and 1.00 Mbar (Si). The calculated RT CTE value for Si, $2.72 \times 10^{-6} \text{ K}^{-1}$, is in good agreement with the corresponding measured value, $2.6 \times 10^{-6} \text{ K}^{-1}$.⁵⁹ The calculated RT CTE for BAs of $3.04 \times 10^{-6} \text{ K}^{-1}$ is close to that of Si. By comparison, for diamond, we obtain $B_0 = 4.42 \text{ Mbar}$ and a RT CTE value of $1.02 \times 10^{-6} \text{ K}^{-1}$, again close to the measured value of $1.1 \times 10^{-6} \text{ K}^{-1}$ ¹⁶⁰ but almost three times smaller than the RT CTE value for Si, suggesting that BAs may be a better candidate for thermal management in Si-based devices than diamond.

H. Other materials?

The findings here suggest that the combination of large $a-o$ gap and acoustic branch bunching should be considered in addition to the four commonly used criteria discussed in Sec. II when searching for high- κ materials. The surprisingly high κ of BAs prompts the question: Are there other materials that also should exhibit anomalously high κ for similar reasons? A seemingly promising prospect is $c\text{-GaN}$. Ga (N) is opposite As (B) across the group IV column of the periodic table, and GaN has a large mass ratio of constituent atoms, which gives a large $a-o$ gap.

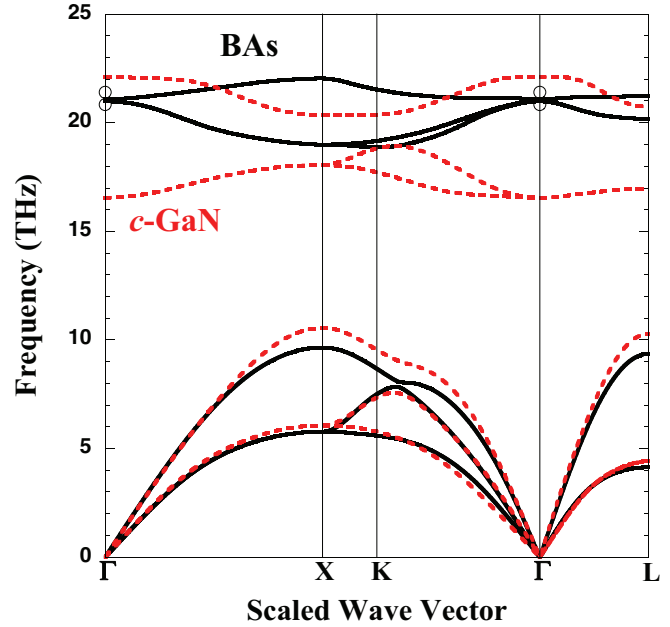


FIG. 11. (Color online) Calculated phonon dispersions for BAs (solid black curves) and $c\text{-GaN}$ (dashed red curves) in the high-symmetry directions. Experimental data for BAs are given by the open black circles.¹⁸

Figure 11 compares the phonon dispersions for BAs and $c\text{-GaN}$. The TA_1 and TA_2 branches almost exactly coincide, and both TA and LA acoustic velocities near the center of the Brillouin zone are similar. However, in the higher acoustic frequency range, the LA branch for $c\text{-GaN}$ lies at higher frequencies, which gives a larger phase space for aaa phonon-phonon scattering and stronger three-phonon scattering matrix elements. Also, $c\text{-GaN}$ has a smaller mass ratio ($M_{\text{Ga}}/M_{\text{N}} = 4.98$) than does BAs ($M_{\text{As}}/M_{\text{B}} = 6.93$), which gives a smaller frequency gap between the TO branches and the acoustic phonons in $c\text{-GaN}$ compared to BAs. This introduces aoa scattering in $c\text{-GaN}$, which is absent in BAs. Further, the calculated anharmonic IFCs of $c\text{-GaN}$ are larger than those of BAs, and these are squared in the three-phonon matrix elements that determine the scattering rates (see eq. 8 in Ref. 5). These differences give increased intrinsic anharmonic scattering rates in $c\text{-GaN}$ compared to BAs. This is illustrated in Figure 12 for the TA_1 branch in each material. As a result, the calculated intrinsic κ of $c\text{-GaN}$, $\kappa_{\text{pure}} = 360 \text{ Wm}^{-1}\text{K}^{-1}$,^{12,14} is almost an order of magnitude smaller than that in BAs.

Further, there is a large isotope mix in $c\text{-GaN}$ on the heavier (Ga) atom, which gives much stronger phonon-isotope scattering rates in $c\text{-GaN}$ than in BAs, as shown in Fig. 13 for the TA_1 phonons in each material. This is in spite of the fact that the mass variance parameter, a multiplicative factor in the isotope scattering rate (see Eq. 6 in Ref. 49), is about seven times larger in BAs. The strong phonon-isotope scattering in $c\text{-GaN}$ gives a large reduction of its intrinsic thermal conductivity to $\kappa_{\text{nat}} = 215 \text{ Wm}^{-1}\text{K}^{-1}$.^{12,14} The significantly lower κ of $c\text{-GaN}$ highlights the sensitivity of the thermal conductivity to the $a-o$ gap, the acoustic branch bunching, the magnitude of the anharmonic IFCs, and the isotope composition of the constituent atoms in each material.

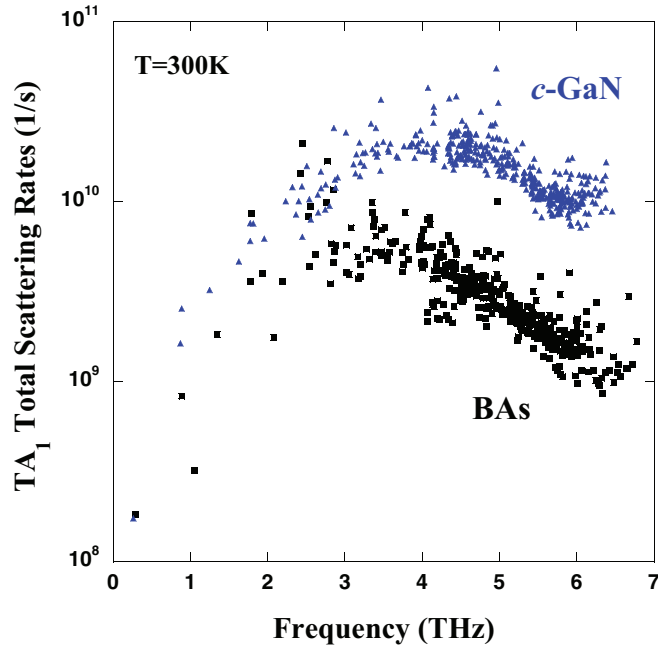


FIG. 12. (Color online) Anharmonic three-phonon scattering rates for the TA_1 branch at $T = 300$ K for BAs (solid black squares) and c -GaN (solid blue triangles) as a function of phonon frequency.

We have examined other cubic and wurtzite group IV, II–VI, and III–V binary systems^{14,48} and have not found any that have a combination of properties as promising as those of BAs. One might expect that group IV and group III–V combinations with large mass ratio would give better prospects than, for example, II–VI materials because of the

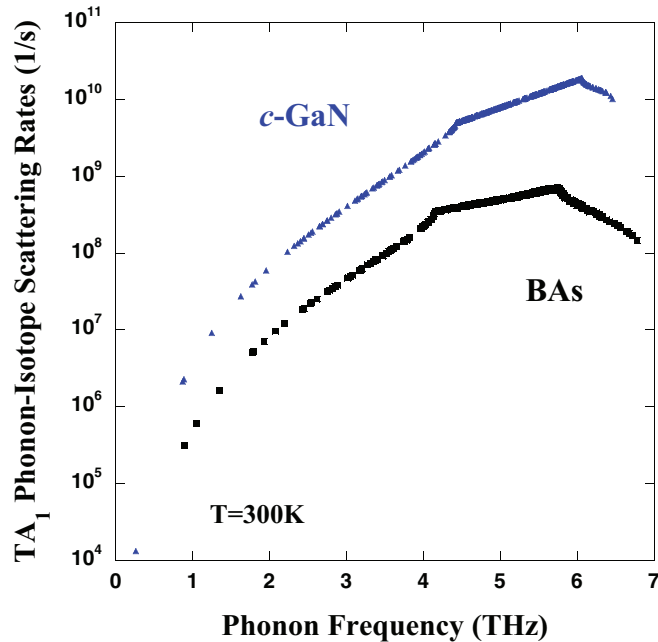


FIG. 13. (Color online) Phonon-isotope scattering rates for the TA_1 branch at $T = 300$ K for BAs (solid black squares) and c -GaN (solid blue triangles) as a function of phonon frequency. c -GaN has larger isotope scattering rates than BAs despite the larger mass variance of boron compared to gallium.

less covalent nature of the latter, which makes for less stiff bonding and lower phonon frequencies. For example, the beryllium chalcogenides, BeSe and BeTe, are qualitatively similar to BAs and BSb in having large a - o gaps and bunching of acoustic branches. However, the calculated intrinsic thermal conductivities are lower.⁴⁸ Nevertheless, the remarkably high κ found for BAs may motivate a systematic examination of large groups of materials, using, for example, recently developed high-throughput approaches.⁶¹

V. SUMMARY AND CONCLUSIONS

In summary, we have used an *ab initio* theory to elucidate the unusual thermal transport properties of BAs that give a calculated RT thermal conductivity, κ_{nat} (κ_{pure}), greater than $2000 \text{ Wm}^{-1}\text{K}^{-1}$ ($3000 \text{ Wm}^{-1}\text{K}^{-1}$) and a value exceeding that of diamond at higher temperatures. The large κ in BAs arises from a combination of vibrational properties, including: bunching together of the acoustic phonon branches, a large mass ratio of the constituent atoms, and an isotopically pure heavy atom, all features not commonly identified as contributing to high κ .

The unusual combination of vibrational properties of BAs results in weak phonon-phonon and phonon-isotope scattering rates and anomalously long acoustic phonon lifetimes in a narrow frequency range resulting in huge RT mean free paths of phonons ($\sim 2 \mu\text{m}$), contributing to κ , with mfp values over two times larger than those for diamond. The resulting sensitivity to scattering of phonons by crystal boundaries necessitates fabrication of large single crystals, preferably at least $10 \mu\text{m}$ in size, in order to avoid large reductions in κ . In addition, high-quality samples with few defects will also be required to observe the predicted ultrahigh κ for BAs.

The large κ predicted from *ab initio* calculations presented here and in Ref. 1 motivates thermal conductivity measurements of high-quality BAs crystals. In addition, the demonstrated sensitivity of the calculated κ to changes in phonon frequencies, anharmonic force constants, and isotope mixture motivates measurements of: (1) the full phonon dispersion for BAs, which would provide useful data about the bunching of acoustic phonon branches, which in turn could be compared with that predicted from *ab initio* calculations.⁶² (2) the CTE for BAs, which would provide information to assess the relatively weak anharmonic force constants calculated from first principles.

For many of the materials that we have examined, κ is sensitive to changes in the vibrational properties. This sensitivity suggests the possibility of further enhancing the κ of BAs and other materials by tuning of these properties. Thus, in principle, manipulation of the chemical bonding in a large mass ratio compound targeted to further bunch together the acoustic branches could drive the thermal conductivity to record high values. Induced strain is potentially one way to accomplish this.

The findings presented here for BAs provide important new insight into the nature of thermal transport in high-thermal-conductivity materials and highlight the need to do fully detailed calculations on phonon physics to understand thermal conductivity even at a qualitative level. The desirable RT coefficient of thermal expansion for BAs, close to that of

silicon, combined with its high- κ value suggest that BAs could be a promising material for use in passive cooling applications.

ACKNOWLEDGMENTS

This work was supported in part by the Office of Naval Research (D.A.B., L.L., and T.L.R.) and DARPA (L.L. and T.L.R.). L.L. acknowledges support from a National Research

Council NRL Research Associateship. D.A.B. acknowledges primary support from the S3TEC, an Energy Frontier Research Center funded by the US Department of Energy, Office of Science, Office of Basic Energy Sciences under Award No. DE-FG02-09ER46577, and also support from the National Science Foundation under Grant No. 1066634. We also thank Natalio Mingo, Jesús Carrete Montaña, Saikat Mukhopadhyay, and Derek Stewart for useful discussions.

- ¹L. Lindsay, D. A. Broido, and T. L. Reinecke, *Phys. Rev. Lett.* **111**, 025901 (2013).
- ²G. A. Slack, *J. Phys. Chem. Solids* **34**, 321 (1973).
- ³D. T. Morelli and G. A. Slack, in *High Thermal Conductivity Materials*, edited by S. Shinde and J. Goela (Springer, New York, 2005), p. 37.
- ⁴D. A. Broido, M. Malorny, G. Birner, N. Mingo, and D. A. Stewart, *Appl. Phys. Lett.* **91**, 231922 (2007).
- ⁵A. Ward, D. A. Broido, D. A. Stewart, and G. Deinzer, *Phys. Rev. B* **80**, 125203 (2009).
- ⁶X. Tang and J. Dong, *Proc. Natl. Acad. Sci. USA* **107**, 4539 (2010).
- ⁷J. Garg, N. Bonini, B. Kozinsky, and N. Marzari, *Phys. Rev. Lett.* **106**, 045901 (2011).
- ⁸K. Esfarjani, G. Chen, and H. T. Stokes, *Phys. Rev. B* **84**, 085204 (2011).
- ⁹J. Shiomi, K. Esfarjani, and G. Chen, *Phys. Rev. B* **84**, 104302 (2011).
- ¹⁰Z. Tian, J. Garg, K. Esfarjani, T. Shiga, J. Shiomi, and G. Chen, *Phys. Rev. B* **85**, 184303 (2012).
- ¹¹Wu Li, L. Lindsay, D. A. Broido, Derek A. Stewart, and Natalio Mingo, *Phys. Rev. B* **86**, 174307 (2012).
- ¹²L. Lindsay, D. A. Broido, and T. L. Reinecke, *Phys. Rev. Lett.* **109**, 095901 (2012).
- ¹³T. Luo, J. Garg, J. Shiomi, K. Esfarjani, and G. Chen, *Europhys. Lett.* **101**, 16001 (2013).
- ¹⁴L. Lindsay, D. A. Broido, and T. L. Reinecke, *Phys. Rev. B* **87**, 165201 (2013).
- ¹⁵J. A. Perri, S. La Placa, and B. Post, *Acta Cryst.* **11**, 310 (1958).
- ¹⁶F. V. Williams and R. A. Ruehrwein, *J. Am. Chem. Soc.* **82**, 1330 (1960).
- ¹⁷S. M. Ku, *J. Electrochem. Soc.* **113**, 813 (1966).
- ¹⁸R. G. Greene, H. Luo, R. Ruoff, S. S. Trail, and F. J. DiSalvo, *Phys. Rev. Lett.* **73**, 2476 (1994).
- ¹⁹S. Wang, S. F. Swingle, H. Ye, F.-R. F. Fan, A. H. Cowley, and A. J. Bard, *J. Am. Chem. Soc.* **134**, 11056 (2012).
- ²⁰R. M. Wentzcovitch, M. L. Cohen, and P. K. Lam, *Phys. Rev. B* **36**, 6058 (1987).
- ²¹J. M. Ziman, *Electrons and Phonons* (Oxford University Press, London, 1960).
- ²²G. Slack, *Solid State Physics*, Vol. 34 (Academic Press, New York, 1979), p. 1.
- ²³G. Leibfried and E. Schlömann, *Nach. Akad. Wiss. Göttingen, Mat. Phys. Klass* **4**, 71 (1954).
- ²⁴C. L. Julian, *Phys. Rev.* **137**, A128 (1965).
- ²⁵For the materials considered here, we have found that $a + o \leftrightarrow o$ processes can provide important contributions to the intrinsic scattering rates but only for relatively low phonon frequencies. Processes of types $a + a \leftrightarrow a$ and $a + a \leftrightarrow o$ represent the dominant scattering channels throughout most of the Brillouin zone.
- ²⁶For the materials considered here, the optic branches are closely spaced, are only weakly dispersive, and reside at higher energies than the acoustic branches. Some materials such as PbTe can have highly dispersive low-lying optic branches with regions in the Brillouin zone below those of portions of the acoustic phonon branches. For such materials, other processes such as $a + o \leftrightarrow a$ are in principle possible.
- ²⁷This is satisfied if all optic modes have frequencies at least twice as large as the highest acoustic mode frequency. Inclusion of momentum conservation can make this condition even more restrictive, eliminating aaa processes even for slightly smaller frequency gaps.
- ²⁸See, for example, C. Kittel, *Introduction to Solid State Physics*, 8th ed. (John Wiley and Sons, Inc., Hoboken, 2005).
- ²⁹We note that κ is sensitive to the interplay of the a - o gap and the acoustic phonon velocities, each of which depends on the heavy atom mass. A larger heavy atom mass acts to reduce κ by lowering the acoustic velocities; however, it also acts to increase κ by giving a larger a - o gap.
- ³⁰M. Lax, P. Hu, and V. Narayanamurti, *Phys. Rev. B* **23**, 3095 (1981).
- ³¹We find numerically that the selection rule removes all phase space for processes of the form $TA_1 + TA_1 \leftrightarrow TA_1$ and $LA + LA \leftrightarrow LA$. So, if all three acoustic branches coincided along either the TA_1 branch or the LA branch, no three-phonon processes could occur. For the more dispersive and anisotropic TA_2 branch, we find a small amount of phase space for $TA_2 + TA_2 \leftrightarrow TA_2$. In principle, if the other two acoustic branches coincided with the TA_2 branch, this would give large but finite phonon lifetimes in the corresponding regions of the Brillouin zone. However, in all other parts of the Brillouin zone away from these regions, the phonon lifetimes as limited by three-phonon scattering would be infinite.
- ³²Higher order processes coupling acoustic and optic phonons would also provide a small amount of thermal resistance.
- ³³For crystals with a single atom per unit cell, only aaa scattering occurs. In such crystals, a bunching of acoustic branches alone could lead to enhanced lattice thermal conductivity.
- ³⁴In the LS theory of Ref. 24, the anharmonicity is characterized by a mode-averaged Grüneisen parameter: $\bar{\gamma} = \sum_{\lambda} C_{\lambda} \gamma_{\lambda} / \sum_{\lambda} C_{\lambda}$, where C_{λ} is the specific heat capacity per phonon mode (see Eq. 2), and the mode Grüneisen parameter, γ_{λ} , is defined in Eq. 6. The calculated RT value of $\bar{\gamma} = 0.67$ for BAs is relatively small compared to many other materials (e.g., see Ref. 3). By comparison, diamond, considered to have weak anharmonicity, has a calculated RT $\bar{\gamma} = 0.75$.

- ³⁵M. Omini and A. Sparavigna, *Nuovo Cimento Soc. Ital. Fis. D* **19**, 1537 (1997).
- ³⁶M. Omini and A. Sparavigna, *Phys. Rev. B* **53**, 9064 (1996).
- ³⁷P. Hohenberg and W. Kohn, *Phys. Rev.* **136**, B864 (1964).
- ³⁸W. Kohn and L. J. Sham, *Phys. Rev.* **140**, A1133 (1965).
- ³⁹S. Baroni, S. Gironcoli, A. D. Corso, and P. Giannozzi, *Rev. Mod. Phys.* **73**, 515 (2001).
- ⁴⁰<http://www.quantum-espresso.org>.
- ⁴¹P. Giannozzi, S. Baroni, N. Bonini, M. Calandra, R. Car, C. Cavazzoni, D. Ceresoli, G. L. Chiarotti, M. Cococcioni, I. Dabo, A. D. Corso, S. Gironcoli, S. Fabris, G. Fratesi, R. Gebauer, U. Gerstmann, C. Gougoussis, A. Kokalj, M. Lazzeri, L. Martin-Samos *et al.*, *J. Phys.: Condens. Matter* **21**, 395502 (2009).
- ⁴²T. Pletl, P. Pavone, U. Engel, and D. Strauch, *Physica B* **263–264**, 392 (1999).
- ⁴³G. Deinzer, G. Birner, and D. Strauch, *Phys. Rev. B* **67**, 144304 (2003).
- ⁴⁴G. Deinzer, M. Schmitt, A. P. Mayer, and D. Strauch, *Phys. Rev. B* **69**, 014304 (2004).
- ⁴⁵J. R. Yates, X. Wang, D. Vanderbilt, and I. Souza, *Phys. Rev. B* **75**, 195121 (2007).
- ⁴⁶Wu Li, Natalio Mingo, L. Lindsay, D. A. Broido, Derek A. Stewart, and N. A. Katcho, *Phys. Rev. B* **85**, 195436 (2012).
- ⁴⁷For our “isotopically pure” calculations, we have omitted the phonon-isotope scattering, while still retaining the isotope-averaged boron mass for simplicity. We have tested the validity of this approximation by calculating κ_{pure} using the isotopically pure boron 11 mass. The phonon dispersions obtained for the two cases are almost indistinguishable, and the phonon-phonon scattering rates are slightly reduced, resulting in a small, 1.5% increase in the BAs thermal conductivity at room temperature (from $3171 \text{ Wm}^{-1}\text{K}^{-1}$ to $3220 \text{ Wm}^{-1}\text{K}^{-1}$).
- ⁴⁸L. Lindsay, D. A. Broido, and T. L. Reinecke, *Phys. Rev. B* **88**, 144306 (2013).
- ⁴⁹S. I. Tamura, *Phys. Rev. B* **30**, 849 (1984).
- ⁵⁰S. Bagci, S. Duman, H. M. Tütüncü, and G. P. Srivastava, *Phys. Rev. B* **79**, 125326 (2009).
- ⁵¹L. Lindsay and D. A. Broido, *J. Phys.: Condens. Matter* **20**, 165209 (2008).
- ⁵²This bunching of acoustic phonon branches also occurs in other materials, such as the beryllium chalcogenide compounds; see Ref. 48.
- ⁵³L. P. Pitaevskii and E. M. Lifshitz, *Physical Kinetics* (Pergamon Press, New York, 1981), p. 287.
- ⁵⁴A. J. Minnich, J. A. Johnson, A. J. Schmidt, K. Esfarjani, M. S. Dresselhaus, K. A. Nelson, and G. Chen, *Phys. Rev. Lett.* **107**, 095901 (2011).
- ⁵⁵J. A. Johnson, A. A. Maznev, J. Cuffe, J. K. Eliason, A. J. Minnich, T. Kehoe, C. M. Sotomayor Torres, G. Chen, and K. A. Nelson, *Phys. Rev. Lett.* **110**, 025901 (2013).
- ⁵⁶K. T. Regner, D. P. Sellan, Z. Su, C. H. Amon, A. J. H. McGaughey, and J. A. Malen, *Nature Comm.* **4**, 1640 (2013).
- ⁵⁷D. A. Broido, L. Lindsay, and A. Ward, *Phys. Rev. B* **86**, 115203 (2012).
- ⁵⁸D. A. Broido, A. Ward, and N. Mingo, *Phys. Rev. B* **72**, 014308 (2005).
- ⁵⁹Y. Okada and Y. Tokumaru, *J. Appl. Phys.* **56**, 314 (1984).
- ⁶⁰S. Stoupin and Y. V. Shvyd'ko, *Phys. Rev. B* **83**, 104102 (2011).
- ⁶¹S. Curtarolo, G. L. W. Hart, M. Buongiorno Nardelli, N. Mingo, S. Sanvito, and O. Levy, *Nat. Mater.* **12**, 191 (2013).
- ⁶²We note that the bunching in the calculated phonon dispersions for diamond shows good agreement with measured data (see Fig. 1 in Ref. 5).